Available online at www.sciencedirect.com

ScienceDirect

Acta Materialia 68 (2014) 61–69

Acta MATERIALIA

www.elsevier.com/locate/actamat

Mechanisms of hydrogen-enhanced localized plasticity: An atomistic study using α-Fe as a model system

J. Song [a,*], W.A. Curtin [b]

[a] Department of Mining and Materials Engineering, McGill University, Montreal, QC, Canada
[b] Institute of Mechanical Engineering, École Polytechnic Fédérale de Lausanne, Lausanne, Switzerland

Received 17 October 2013; received in revised form 2 January 2014; accepted 3 January 2014
Available online 12 February 2014

Abstract

Atomistic simulations of the effects of H on edge dislocation mobility and pile-ups are performed to investigate possible nanoscale mechanisms for hydrogen-enhanced localized plasticity (HELP). α-Fe is used as a model system because H diffusion is fast enough to capture kinetics within the time scales of molecular dynamics and because edge dislocation glide in α-Fe is similar to glide in face-centered cubic metals. Results over a wide range of H concentrations sufficient to generate a range of sizes in the Cottrell atmospheres show that the Cottrell atmospheres follow the moving dislocations, leading to a resistance to dislocation motion that is consistent with solute drag theory; thus, H reduces the dislocation mobility. Furthermore, once motion stops and a pile-up is established, the H Cottrell atmospheres do not affect the equilibrium spacing of dislocations in the pile-up; thus, the H atmosphere provides no "shielding" of dislocation–dislocation interactions. This result is consistent with conclusions from previous continuum calculations. Two oft-proposed mechanisms for HELP (H-induced increase in true dislocation mobility and decrease in dislocation–dislocation pile-up interactions) are therefore not supported by the present simulations. A mechanistic understanding of HELP phenomena observed in various experiments thus requires evaluation of more complex H–dislocation interactions.

Keywords: Hydrogen embrittlement; Dislocation pile-up; Atomistic simulations; Solute drag

1. Introduction

Hydrogen embrittlement (HE) has been a consistent problem in the application of metals in industrial settings for decades [1–4]. Despite intense research efforts, the exact mechanisms of HE remain far from being universally accepted. Various mechanisms in the literature include hydrogen-enhanced decohesion [5–10], hydrogen-enhanced local plasticity (HELP) [11–13], and hydride formation and cleavage [14–16]. We have recently developed a predictive nanoscale mechanism for HE in which the aggregation and transport of H atoms around a crack tip can inhibit dislocation emission to induce a local "ductile-to-brittle" transition, followed by sustainable slow crack growth [17,18]. While explaining some aspects of embrittlement, it does not address other phenomena that are influenced by H, such as HELP. Here, we focus on possible HELP mechanisms independent of their possible roles in embrittlement.

HELP is supported primarily by experimental observations of enhanced dislocation motion [19–21] and localized slip bands in the vicinity of the crack tip in H-charged test specimens [22,23]. The HELP mechanism is also widely quoted to interpret macroscopic measurements of reduced material yield stress [24] and other softening phenomenon [25,26] in the presence of H, as well as the easier dislocation nucleation observed during indentation experiments with

* Corresponding author.
E-mail address: jun.song2@mcgill.ca (J. Song).

http://dx.doi.org/10.1016/j.actamat.2014.01.008
1359-6454/$36.00

in situ or ex situ H charging [27,28]. However, there remain contradictory results, such as increases in flow stress in the presence of H in Ni [29], Al [30] and Fe alloys at high strains [31–34]. The range of experimental observations of HELP phenomena clearly merit a mechanistic understanding at microscopic scales.

Two mechanisms have commonly been postulated to cause the observed HELP phenomena: (i) H increases dislocation mobility, leading to material softening [26,35,36]; and (ii) H reduces dislocation–dislocation interactions, which facilitates planar slip and increases pile-up phenomena that lead to damage initiation [37–39]. Small-scale experiments using in situ transmission electron microscopy (TEM) on samples deformed in tension [19] indicate, however, that neither of these mechanisms directly operates. The authors of Ref. [19] suggested a third mechanism: (iii) H modification of dislocation pinning phenomena, i.e. H interacts with other defects to modify the ability of those defects to impede dislocation motion. Mechanisms analogous to (ii) and (iii) were investigated theoretically using continuum models by Sofronis et al. [11,40–43], in which it was shown that mechanism (ii) is unlikely and mechanism (iii) plausible, while mechanism (i) is not amenable to continuum-level analysis. In addition, there have been studies, based on H reducing the vacancy formation energy, that suggest H charging induces high concentrations of hydrogen-stabilized vacancies, i.e. H–vacancy complexes, possibly also contributing to the operation of mechanism (iii) [44–49]. Nonetheless, mechanisms (i) and (ii) remain commonly quoted in the current literature as viable mechanisms for HELP and continue to be studied [50–53]. As a result, we are motivated to examine HELP mechanisms (i) and (ii) using atomistic simulations that accurately capture the dislocation/H interactions including kinetic effects.

Specifically, we study the motion/mobility of dislocations and the structure of edge dislocation pile-ups in Fe in the absence and presence of dissolved H. Although the TEM experiments are performed on face-centered cubic (fcc) Al and austenitic stainless steel, we use body-centered cubic (bcc) Fe as a model system because the kinetics of H transport in Fe is fast enough to be captured in molecular dynamics and because the edge dislocation in Fe has a dissociated core structure and a low Peierls barrier [54,55] and so has characteristics typical of edge dislocations in fcc metals. We use large-scale molecular dynamics (MD) simulations with sufficiently long times to place some bounds on the possible effects of very slow kinetic processes that are difficult to address in nanosecond-scale MD simulations. We find that the effect of H on dislocation mobility is consistent with standard solute drag theory, in which mobility is inhibited by an atmosphere of H that diffuses with the moving dislocation. We also find that a three-dislocation pile-up of straight, parallel edge dislocations in Fe under a wide range of applied loads and H concentrations has a structure (i.e. spacing of pile-up dislocations) that is independent of whether or not H is present, and is independent of the details of how the system reaches the final equilibrium structure. Neither of these simulations reveals any phenomena associated with softening in the flow or dislocation interactions. These results indicate that the experimental TEM observations of the behavior of dislocation pile-ups upon introduction of H is not due to any modifications to the "shielding" of the dislocation interactions by the H atmospheres [19], consistent with the conclusions of Sofronis et al. [11]. This work should put to rest the viability of mechanisms (*i*) and (*ii*) such that future work can focus on other possible mechanisms for HELP.

2. Computational methodology

We construct a rectangular simulation cell comprised of a bcc Fe crystal oriented as $X = [1\,1\,1]$, $Y = [1\,\bar{1}\,0]$ and $Z = [1\,1\,\bar{2}]$, and of dimensions $L_x = 39.6$ nm, $L_y = 38.8$ nm and $L_z = 2.8$ nm. Within the simulation cell, we place three equally spaced edge dislocations, all having Burgers vector $\frac{1}{2}[111](1\,\bar{1}\,0)$ and line direction along Z, onto the central $(1\,\bar{1}\,0)$ plane, as illustrated in Fig. 1a. The edge dislocations are created by removing atoms from the perfect crystal in the band $-\sqrt{3}a_0/4 < X - X_i < \sqrt{3}a_0/4, Y < 0$, where $a_0 = 2.86$ Å is the lattice constant for α-Fe and X_i is the X coordinate of the ith dislocation. We then displace the surrounding atoms according to the linear elastic displacement fields for the edge dislocation [56], and relax the entire structure using the conjugate gradient method [57]. We use an edge dislocation pile-up to maximize the H–dislocation interaction effects, and because edge glide is similar to glide in fcc materials, as noted above. As a practical matter, the screw-dislocation–H interactions predicted with the interatomic potential employed here exhibit some unphysical local effects that would also make such a study invalid. A dislocation obstacle is created along the slip plane at

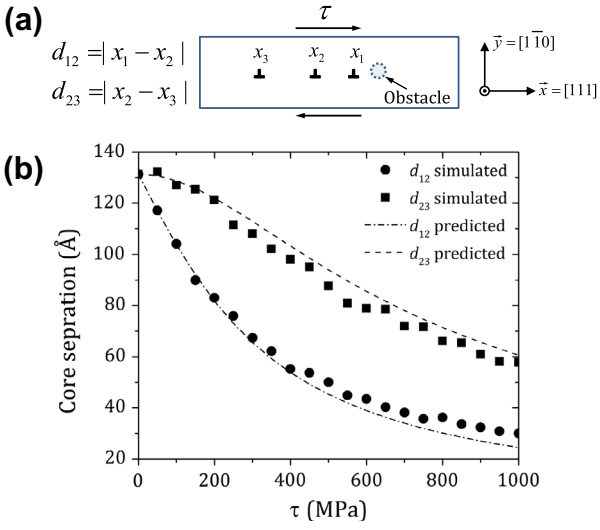

Fig. 1. (a) Schematic of dislocations heading toward, and piling up at, an obstacle when subject to a shear stress τ. (*b*) Simulated and predicted (Eq. (4)) separations between dislocation cores under shear stress τ at $T = 500$ K in pure Fe (no H).

$X = 18$ nm by freezing atoms within a cylindrical region parallel to Z and of radius 6 Å.

The simulation cell is periodic along the Z direction (but with a relatively large 2.8 nm periodic length) and free along the Y direction. The periodicity along the Z direction effectively enforces a plane-strain boundary condition along the dislocation line direction. Periodic boundary conditions are also enforced along the X direction without removing any end atoms. Since the slip and long-range strain fields introduced by dislocations are incompatible with periodic boundary conditions perpendicular to the dislocation line, this necessarily introduces some artificial bending stresses that do not exist for an array of dislocations in an infinite box. Nonetheless, the bending stresses do not produce any shear stress along the slip plane, and hence do not influence the result here.

Starting from the initial simulation cell without H, H atoms are introduced by randomly inserting them into tetrahedral sites in the region >1 nm away from free surfaces to create various H-charged atomic configurations. Two reflecting boundaries[1] are also imposed for H atoms, located at 1 nm from the surfaces, to prevent H from artificially segregating to the free sample surfaces. The degree of H charging is prescribed by the bulk H concentration c_0 as follows. For α-Fe crystal at temperature T and a bulk equilibrium H concentration c_0 (related to an imposed H chemical potential) defined here on a per Fe atom basis, an H atom will diffuse due to the driving force $p\Omega$ created by the interaction of the pressure field of the dislocation at x_i, $p(x - x_i, y)$, with the misfit volume Ω of the H atom. The chemical potential in the presence of the field, neglecting H–H interactions and within simple solution theory, is given by the general expression:

$$\mu = \mu_0 + k_B T \ln \frac{c}{1-c} + p\Omega; \quad p(r,\theta) = -\frac{(1+\nu)Gb}{3\pi(1-\nu)}\frac{\sin\theta}{r}, \tag{1}$$

where G is the shear modulus, $b = \sqrt{3}a_0/2$ is the magnitude of the Burgers vector, and (r, θ) are the polar coordinates around a dislocation located at the origin. Since the chemical potential is constant throughout the system, the local concentration c at position (r, θ) around a single dislocation is given by solving Eq. (1) and exchanging the chemical potential for the bulk far-field concentration as:

$$c(r,\theta) = \frac{c_0 \exp\left(\frac{p\Omega}{k_B T}\right)}{1 + c_0 \exp\left(\frac{p\Omega}{k_B T}\right)}. \tag{2}$$

The total number of H additional atoms N_H at equilibrium within a cylindrical volume of radius R and thickness Z_0 around the edge dislocation as a function of c_0 is then:

$$N_H(c_0) = Z_0 \int_0^{2\pi}\int_0^R \left[\frac{c_0 \exp\left(\frac{p\Omega}{k_B T}\right)}{1 + c_0 \exp\left(\frac{p\Omega}{k_B T}\right)} - c_0\right] r dr d\theta. \tag{3}$$

By setting $R = d/2$, where d is the initial dislocation spacing in the system, Eq. (3) allows us to estimate the total amount of H needed in the simulation cell such that all the H in the cell will participate in any Cottrell atmosphere around the dislocations spaced by d at bulk concentration c_0. In an infinite system, H would be attracted to a static pile-up from infinite distances, and so we must recognize there is no well-defined "true" equilibrium configuration. For our simulations, $\Omega = 3.818$ Å^3 and, with three dislocations in the simulation cell, a total of $3N_H$ (c_0; $R = d/2$) H atoms are introduced into the system.

Fig. 2 shows the amount of H per unit length of dislocation line, i.e. N_H/L_z along the dislocation line direction, that should be introduced into the simulation cell as a function of the "far field" concentration c_0 at various temperatures T. Values of N_H/L_z used in our simulations ranges from 7.1 to 36.4 nm^{-1}, as indicated by the gray area in Fig. 2. Simulations at any given level of N_H/L_z are thus sufficient to generate Cottrell clouds at a range of far field concentrations and temperature (c_0, T). In practice, we examine a series of H concentrations c_0 ranging from 0.075% to 2% at $T = 500$ K, where the temperature facilitates the diffuse transport of H and the motion of any Cottrell atmospheres over time scales observable in MD simulations. However, Fig. 2 shows that the amount of H added in these simulations is the same as the amount that would be added at $T = 300$ K for concentrations between 10^{-5} and 2×10^{-3}, which are in the range of experimental concentrations expected in various metals. Therefore, the use of $T = 500$ K is quite acceptable for the purposes of examining the oft-used interpretations for the HELP, i.e. H-shielding dislocation–dislocation interactions and H effects on mobility.

We note that we do not accommodate the H-induced expansion in our simulations and thus the simulation box with higher H content is subject to higher normal pressures across the periodic boundaries. Nonetheless several

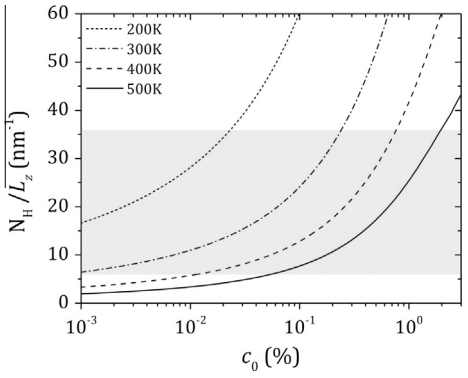

Fig. 2. Amount of H per unit length, N_H/L_z, along the dislocation line for an edge dislocation in α-Fe, as a function of the bulk far-field H concentration c_0, for different temperatures. The gray area indicates the range of N_H/L_z considered in the current simulations.

[1] The reflecting boundary is implemented as follows: at any instantaneous time t, if an H atom is projected to cross it moving towards the free surface in the next timestep, then the instantaneous displacement d and velocity v of the atom will be changed to $-d$ and $-v$, respectively.

benchmark simulations where H-induced expansion is accommodated have been performed, showing no noticeable change in pile-up configurations.

The MD simulations are performed in an NVT ensemble with a Nosé–Hoover thermostat [58,59] and velocity–Verlet algorithm [60] with the integration time steps being 0.4 and 2 fs for the pure Fe sample and H-charged samples, respectively. The interatomic interactions among atoms are described using a Finnis–Sinclair-type [61] embedded atom method (EAM) potential that has been modified to prevent unphysical H–H aggregation [62–64]. This potential matches many key properties of the Fe–H system with no serious deficiencies aside from a spurious interaction in the core of the screw dislocation, which is explicitly not studied here. Tractions are applied on the surfaces normal to the Y direction to drive dislocation motion. The dimension along the Y direction is large enough to minimize the influence of the free (traction) surfaces on the dislocation pile-up, i.e. on the resolved shear stresses created by the dislocations along the glide plane (see Supplementary Data). The presence of free surfaces also affects the hydrostatic stress field, leading to deviations from the bulk pressure field. The largest deviations (for the hydrostatic stress and any normal stresses) occur near the free surfaces and are of the order of 100 MPa, producing an error in the energy of an H atom of ~0.002 eV, which is negligible for the range of bulk H concentration c_0 considered in this study. Furthermore, such deviations are negligible in the vicinity of the dislocation core.

For each simulation, the system is first equilibrated at $T = 500$ K for a total of ~2 ns, after which forces of equal magnitude but opposite sign are applied to atoms located within the atomic potential [64] cut-off radius of the Y surfaces to generate the shear stress τ. The applied shear stress drives the dislocations to pile-up against the obstacle. The shear stress is applied in two ways, in a single pulse or using step-loading. When τ is applied in a pulse, the system is relaxed for ~20 ns following the application of τ to obtain an equilibrium dislocation pile-up configuration. For the step-loading, τ is incremented in steps of 50 MPa until the desired load level is reached. Between loading steps, the system is relaxed for 2 ns for pure Fe and 4 ns for Fe–H systems, respectively. For a particular τ, no difference in the equilibrium pile-up configurations is observed for the two methods of applying stress.[2] Note that after applying the stress, the simulations are run at constant stress for an extended period of time so that we are studying a near-equilibrium situation over the simulation time scales, and there is no equivalent "strain rate" in these simulations.

[2] It is worth noting that pulse loading may result in "temporary" break-away of the second and/or third dislocations if the applied stress is sufficiently large. In this scenario, the dislocation will quickly resettle following the initial break-away to a position closer to its immediate neighbor on the right, after which H atoms will migrate to the new position to form a H cloud around the dislocation core again. This temporary break-away of dislocation(s) does not influence the equilibrium pile-up configuration though it may result in significant uneven distribution of H atoms at different dislocation cores.

3. Results and discussion

3.1. Pure Fe: pile-up configurations and mobility

We first examine the pure Fe system, which will serve as a reference for the behaviors in the Fe–H system. Note that this case includes all image interactions due to periodicity and free surfaces, and so is a precise reference case when considering the effects of added H. We denote the horizontal separation between the ith and jth dislocations as d_{ij} $(i,j = 1,2,3)$, defined as $d_{ij} = |x_i - x_j|$ with x_i and x_j being the x coordinates of the centers of the ith and jth dislocations. Upon application of the applied stress, the dislocations accelerate and then move at high velocity (e.g. ~750 m s^{-1} at 200 MPa, see Supplementary Data) and then decelerate and come to rest in an equilibrium pile-up configuration. The equilibrium separations d_{12} and d_{23} as functions of the applied stress τ, as found in our simulations, are shown in Fig. 1b. The separation distances d_{12} and d_{23} can be accurately estimated from isotropic continuum theory by balancing the net force on the second and third dislocations as:

$$\begin{aligned} 2^{\text{nd}}\perp&: \sum_{n=0}^{\infty}\left(\frac{A}{nL_x - d_{12}} + \frac{A}{nL_x + d_{23}}\right) - \sum_{n=1}^{\infty}\left(\frac{A}{nL_x + d_{12}} + \frac{A}{nL_x - d_{23}}\right) + \tau = 0; \\ 3^{\text{rd}}\perp&: \sum_{n=0}^{\infty}\left(\frac{A}{nL_x - d_{12} - d_{23}} + \frac{A}{nL_x - d_{23}}\right) - \sum_{n=1}^{\infty}\left(\frac{A}{nL_x + d_{12} + d_{23}} + \frac{A}{nL_x + d_{23}}\right) + \tau = 0; \end{aligned} \tag{4}$$

where $A = \frac{Gb}{2\pi(1-v)}$ and the infinite summations are contributions from the periodic images of the dislocations. In the Supplementary Data, we have shown that with the sufficiently large cell dimensions used in our simulations the influence due to free surfaces on the shear stress along the dislocation glide plane is negligible. For α-Fe, $v = 0.29$ and $G = 72.56$ GPa at $T = 500$ K (Voigt averages [65]), the isotropic continuum predictions of d_{12} and d_{23} from Eq. (4) are also shown in Fig. 1b and there is excellent agreement over the entire range of applied stresses, with deviations <5 Å. This comparison verifies that the image stresses due to the traction boundary condition are negligible.

3.2. Hydrogen aggregation and solute drag

For systems pre-charged with H, the H atoms form highly concentrated clouds around each dislocation core after relaxation, as shown in Fig. 3a and b and as anticipated by the attractive H–dislocation interaction. Fig. 3b that shows that H atoms, having a positive misfit volume, accumulate on the side of the dislocation that is under tensile pressure, as expected. We note that the trapping energy of H in the edge dislocation core is ~0.4 eV, broadly comparable to the trapping energy of H neighboring a single vacancy that ranges from 0.1 to 0.6 eV [64]. The H atoms are densely packed into a Cottrell cloud within a region of a few nanometers around the dislocation core.

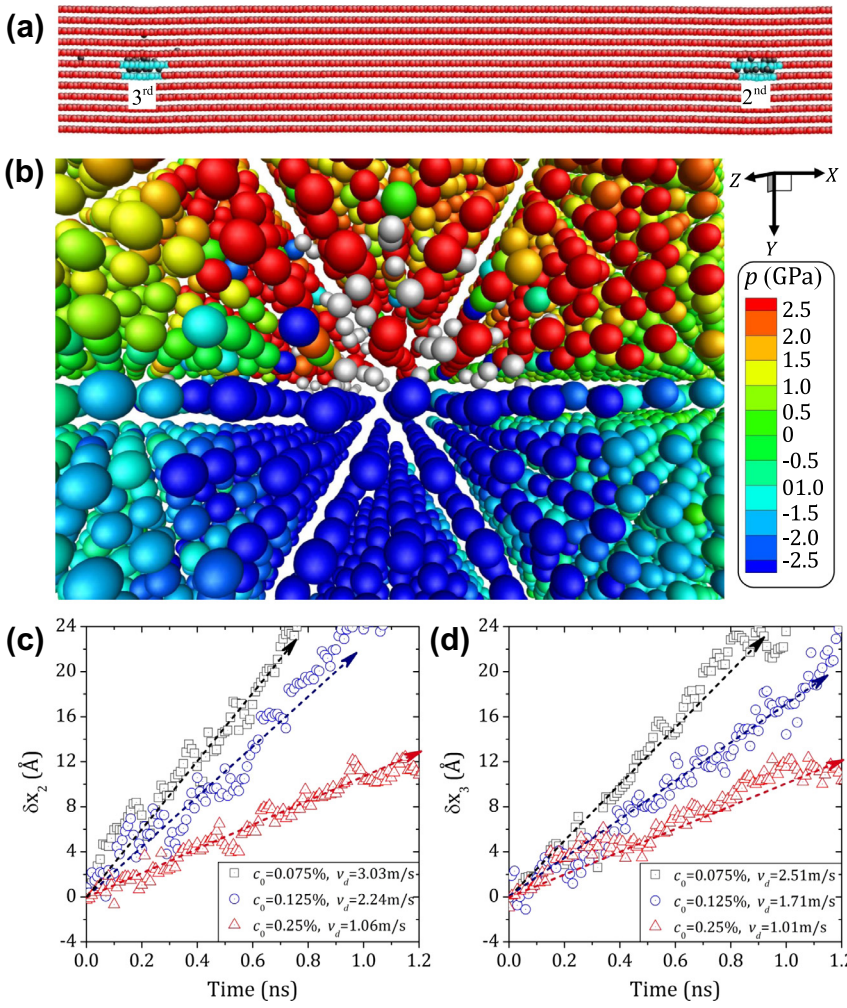

Fig. 3. (a) Projected atomistic view (along the Z direction) of the second and third dislocation cores surrounded by clouds of H atoms (H atoms, black; Fe atoms in dislocation core, cyan; other Fe atoms, red). (b) Close-up perspective atomistic view of a dislocation core surrounded by the cloud of H atoms that form naturally in the simulation, at $c_0 = 2\%$ (H atoms, silver; Fe atoms colored via the pressure field p, with positive and negative values indicating tension and compression respectively). (c, d) Time evolution of the x-coordinate for the second and third dislocation cores within the first 1.2 ns after application of $\tau = 400$ MPa, for materials with three representative H concentrations c_0 as indicated. The corresponding dislocation velocities v_d (i.e. the slopes of curves) are also noted. (For interpretation of the references to color in this figure legend, the reader is referred to the web version of this article.)

Under the application of the applied shear, the dislocations are driven to pile-up against the obstacle. During the motion of the dislocations, the H atmosphere travels along with the dislocation via diffusion and exerts a substantial resistance to dislocation motion due to solute drag. Fig. 3 shows the positions of the second and third dislocations vs. time during the 1.2 ns immediately after the application of a pulse stress of $\tau = 400$ MPa.[3] During the first 1.2 ns, the dislocation velocities v_d are nearly constant at the values noted in Fig. 3. These velocities scale nearly inversely with the H concentration c_0 and, on the order of 1 m s^{-1}, are orders of magnitude smaller than the velocities of the dislocation in pure Fe. The substantially lower dislocation velocity in the presence of H suggests that the dislocation motion is largely controlled by the H kinetics. In fact, the motion of the dislocations in Fe–H is generally consistent with solute drag [66,67], in which the dislocation velocity is governed by a balance between the applied driving force and the retarding force of the H cloud that is able to diffuse along with the dislocation. Solute drag is observable here because the activation barrier for diffusion of H in Fe is very low (~0.04 eV) so that diffusion phenomena can be observed on the time scales of molecular dynamics simulations [68]. To our knowledge, this is the first explicit atomistic simulation of solute drag and this is the first main result of this paper.

We now make some quantitative comparisons of the measured dislocation motion with the predictions of solute drag theory [55,68,69]. In the regime of steady drag, the relationship between dislocation velocity and applied shear stress is predicted to be:

$$\tau = v_d c_0 \left(\frac{\beta^2}{D v_a b k T} \right), \tag{5}$$

[3] For all the cases examined, dislocation break-away did not occur.

where D is the bulk solute diffusion coefficient, v_a is the host atomic volume, b the Burgers vector, and β a material parameter related to the strength of the solute–dislocation interaction. Fig. 4 shows the product $v_d c_0$ (where v_d is the average velocity over the initial $\delta t = 1.2$ period) vs. the applied pulse stress τ for the second and third dislocations. The results clearly exhibit the linear relationship between $v_d c_0$ and τ as predicted by solute drag theory, for various concentrations, a range of stress levels, and with the same linear relationship obtained for both the second and third dislocations in the pile-up. This confirms the operation of solute drag.

Solute drag is quantifiable at the start of these simulations because, during this time, the net applied force on each dislocation is equal to the applied force. After a small amount of motion, the pile-up starts to form and non-periodic dislocation–dislocation interactions occur, so that the stresses on the dislocations are no longer constant with time and the dislocations decelerate as they approach their new equilibrium positions. Therefore, it is not possible to evaluate the solute drag behavior after a few nanoseconds, when the dislocations start slowing down. Deviations can also exist at small applied loads, where the net distance moved is so short that the there is no region of steady-state motion to evaluate. Finally, more quantitative comparisons with solute drag theory, such as achieved for Al–Mg [68], are not available because the results can depend on subtle details of H–core interactions where the core "diffusion" might deviate substantially from the bulk diffusion of H in Fe under the influence of local stresses and H–H interactions [70].

From the above observations, we conclude that the direct H effect on edge dislocation mobility is solute drag, i.e. H reduces the mobility of the edge dislocation. Here, the term "mobility" represents the intrinsic or fundamental mobility of a dislocation (with or without solute drag), and should not be confused with an experimentally measured effective mobility that represents the average velocity of a dislocation as it moves via thermal activation past obstacles. This is the second main result of this paper.

3.3. Effects of hydrogen on pile-up configurations

After the dynamic phase of the simulation, the dislocation pile-up reaches a new equilibrium configuration. Fig. 5 shows the values of the separation distances d_{12} and d_{23} in the equilibrium configurations at two representative shear stresses, $\tau = 200$ MPa and 400 MPa, for different c_0, as measured over times of ~5 ns after attaining the equilibrium positions. Within the accuracy of the thermal vibrations of the dislocation line, which occur even at zero H concentration (pure Fe), the pile-up configurations are identical in all cases. This conclusion holds regardless of the method of loading. There is absolutely no tendency for the H atmospheres to have any influence on the dislocation spacings in the pile-up at any applied load or any H concentration, i.e. there is no apparent shielding effect of H on dislocation–dislocation interactions. This is the third main result of this paper.

The experimental observations of H-induced changes in dislocation pile-up behaviors are therefore not caused by fundamental changes in the dislocation–dislocation interactions caused by H. The absence of any "shielding" effect due to the H atmosphere is not surprising when considered from a mechanics viewpoint. The region of material containing the H atmosphere near the dislocation core can be viewed as an inclusion having a transformation strain $\boldsymbol{\varepsilon}^T$ due to the local volume expansion induced by H atoms. The stress fields outside of an inclusion of characteristic in-plane dimension R and infinite in the out-of-plane dimension scale as $|\varepsilon^T|(R/r)^2$ [71]. The resolved shear stresses associated with the H atmosphere thus decay much faster than the dislocation fields, which scale as $1/r$. Thus, the H atmosphere is expected to have negligible effects on the dislocation positions unless the H atmosphere has dimensions R that are approaching the dislocation spacing itself. Fig. 1b shows that at typical applied stresses, the dislocation spacings in the three-dislocation pile-up remain fairly large (~50 Å), much larger than even the largest Cottrell atmospheres studied here (Fig. 3). The dislocation spacings studied here are also much smaller than those observed in

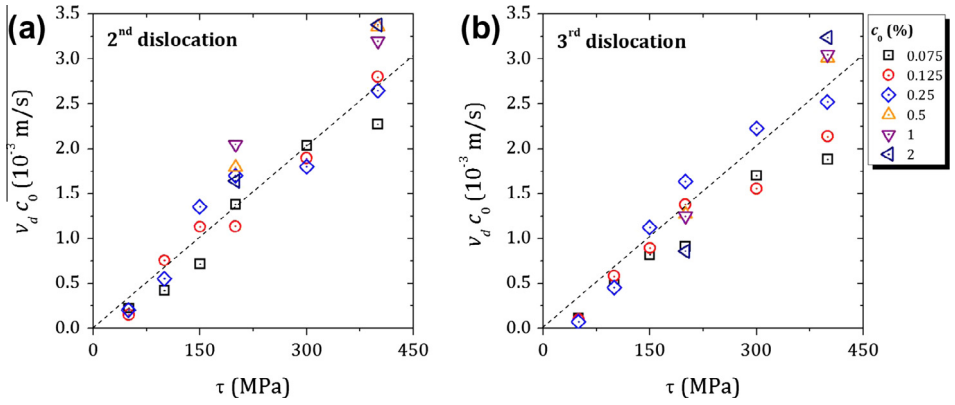

Fig. 4. Product $v_d c_0$, as computed from the atomistic trajectories of the dislocation cores (see Fig. 3), as a function of the applied pulse stress τ for (*a*) the second and (*b*) the third dislocation in the pile-up, showing a linear scaling consistent with predictions of solute drag theory. The dashed lines in (a) and (b) are identical, illustrating that the evolution of $v_d c_0$ vs. τ follows the same trend for the second and third dislocations.

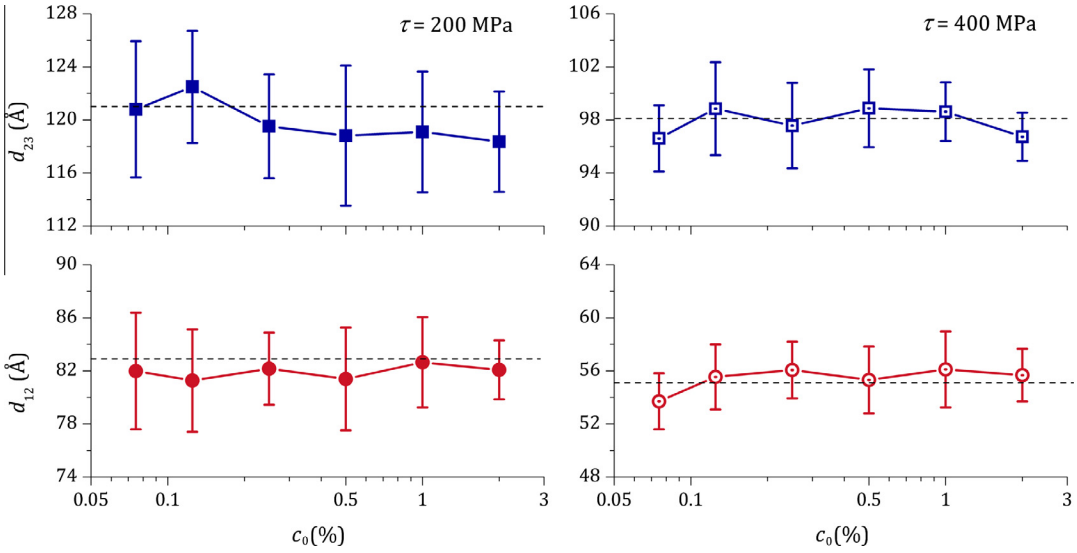

Fig. 5. Equilibrium dislocation separations d_{12} and d_{23} under applied stresses $\tau = 200$ and 400 MPa for systems with different H concentrations c_0. The dashed line in each sub-figure indicates the corresponding d_{12} or d_{23} in the pure Fe system ($c_0 = 0$). Error bars reflect the range of positions measured, as caused by thermal motion of the dislocation. Within thermal noise, the presence of H has no effect on the dislocation spacings in the pile-up at any stress and any H concentration studied here.

the TEM experiments, and so should show larger effects, if such effects exist, than in the experiments. The conclusion from our atomistic studies that there is no shielding due to H clouds for moderately spaced dislocations agrees with the conclusion reached by Sofronis et al. [11,72] using a continuum analysis of a two-dislocation pile-up. Recent computations of the stress field around an edge dislocation in Ni having a Cottrell H atmosphere (created by other means) also lead to the conclusion that dislocation–dislocation interactions are negligible for dislocation separations on the order of 50 Å or larger (as here and in the experiments).

3.4. Discussion

There is obvious TEM evidence that when H is introduced into the chamber of a microscope holding a sample containing a dislocation pile-up that the dislocations move closer together [19,20]. When the H is extracted from the chamber, the dislocations may (in Al) or may not (stainless steel) move back close to their original positions. Our study of a pile-up with H under constant applied stress shows no evidence of these effects. The authors of the experimental work speculated, via detailed examination of the dislocation pile-ups, that H was not directly connected to changes in mobility or dislocation interactions. Our results are consistent with the deduced absence of mobility or shielding effects, i.e. mechanisms (i) and (ii) discussed in the Introduction are not operative. We cannot rule out that some very slow long-range H transport among the dislocation cores might change the pile-up structure over time scales much longer than we can simulate (tens of nanoseconds). However, there is no clear driving force for such a process—the H clouds around each individual dislocation are stable low-energy configurations and so transferring H from one cloud to another should increase the total energy of the system. In addition, the dislocations are also already sitting in positions dictated by their long-range interactions independent of the presence of the H. Thus, the conclusion drawn here on quasistatic configurations over the nanosecond time scale would seem to be valid on much longer time scales. The authors of the experimental study further concluded that H was mainly influencing some unidentified dislocation pinning (mechanism (iii) in the Introduction) and this mechanism is not investigated here.

4. Conclusions

We have investigated the possible role of H in influencing edge dislocation mobility and pile-up structures in Fe, as a means of assessing oft-proposed mechanisms for HELP. Our molecular simulations show that H forms Cottrell atmospheres around moving dislocations, causing solute drag and therefore resisting rather than facilitating dislocation motion. Furthermore, our simulations show that the pile-up structure, under an applied load, is independent of the presence of H, so that the H atmosphere provides no measurable shielding of dislocation interactions. While our simulations are on Fe–H and edge dislocations, the phenomena observed are expected to be common to other metals with easy non-thermally-activated glide, particularly elemental fcc metals such as Al or Ni. Our results indicate that two oft-proposed mechanisms for HELP are not operative, which are the conclusions previously drawn from TEM observations of dislocation pile-ups in H-charged metals (Al and stainless steel) and from continuum modeling. Thus, other mechanisms for HELP

must be developed and examined in more detail. Since macroscopic softening (reduced flow stress) is observed in some metals when charged with H [26,73,74], we expect that such softening is due to interactions of H with other defects (solutes, precipitates, forest dislocations) that otherwise serve to inhibit dislocation motion. Other mechanisms, such as H interactions within the cores of screw dislocations that facilitate kink-pair formation and thus dislocation motion, are feasible but are not likely in fcc materials (Al, Ni, austenitic stainless steels) where HELP effects have often been reported. While molecular simulations remain limited due to (i) availability of sufficiently accurate metal–H interatomic potentials and (ii) diffusional time scales in most metals, where H migration barriers are often on the order of 0.5 eV [64], targeted MD studies such as those presented here can help assess the feasibility of nanoscale mechanisms of HELP.

Acknowledgement

The authors acknowledge partial support of this work by the NSERC Discovery Grant (Grant No. RGPIN 418469-2012).

Appendix A. Supplementary material

Supplementary data associated with this article can be found, in the online version, at http://dx.doi.org/10.1016/j.actamat.2014.01.008.

References

[1] Merrick RD. Mater Performance 1989;28:53.
[2] Rhodes PR, Skogsberg LA, Tuttle RN. Corrosion 2007;63:63.
[3] Rogers HC. Science 1968;159:1057.
[4] Comer JC. Choice Curr Rev Acad Libraries 2005;42:1053.
[5] Troiano AR. Trans ASM 1960;52:54.
[6] Gerberich WW, Marsh P, Hoehn J, Venkateraman S, Huang H. In: Magnin T, Gras JM, editors. Proc int conf on corrosion–deformation interactions; 1993. p. 633.
[7] Oriani RA, Josephic PH. Acta Metall Mater 1974;22:1065.
[8] Gerberich WW, Foeche TJ. Hydrogen enhanced decohesion in Fe–Si single crystals: implications to modelling of thresholds. In: Moody NR, (Eds.), *Hydrogen effects on material behaviour*, Warrendale, PA: TMS; 1990. p. 687.
[9] Oriani RA. Ber Bunsen-Ges Phys Chem 1972;76:848.
[10] Gerberich WW, Marsh PG, Hoehn JW. Hydrogen induced cracking mechanisms—are there critical experiments? In: Moody NR, Hoehn JW, editors. Hydrogen effects in materials. Warrendale, PA: TMS; 1996.
[11] Birnbaum HK, Sofronis P. Mater Sci Eng A Struct Mater Prop Microstruct Process 1994;176:191.
[12] Beacham CD. Metall Mater Trans B 1972;3:437.
[13] Robertson IM. Eng Fract Mech 2001;68:671.
[14] Westlake DG. Trans ASM 1969;62:1000.
[15] Gahr S, Grossbeck ML, Birnbaum HK. Acta Metall Mater 1977;25:125.
[16] Shih DS, Robertson IM, Birnbaum HK. Acta Metall Mater 1988;36:111.
[17] Song J, Curtin WA. Acta Mater 2011;59:1557.
[18] Song J, Curtin WA. Nat Mater 2013;12:145.
[19] Ferreira PJ, Robertson IM, Birnbaum HK. Acta Mater 1998;46:1749.
[20] Ferreira PJ, Robertson IM, Birnbaum HK. Acta Mater 1999;47:2991.
[21] Sofronis P, Robertson IM. Philos Mag A Phys Condens Matter Struct Defects Mech Prop 2002;82:3405.
[22] Murakami Y. Int J Fract 2006;138:167.
[23] Abraham DP, Altstetter CJ. Metall Mater Trans A 1995;26:2859.
[24] Teter DF, Robertson IM, Birnbaum HK. Acta Mater 2001;49:4313.
[25] Matsui H, Kimura H, Kimura A. Mater Sci Eng 1979;40:227.
[26] Matsui H, Kimura H, Moriya S. Mater Sci Eng 1979;40:207.
[27] Gerberich WW, Stauffer DD, Sofronis P. Eff Hydrogen Mater 2009:38.
[28] Barnoush A, Vehoff H. Eff Hydrogen Mater 2009:187.
[29] Boniszewski T, Smith GC. Acta Metall Mater 1963;11:165.
[30] Watson JW, Shen YZ, Meshii M. Metall Trans A Phys Metall Mater Sci 1988;19:2299.
[31] Asano S, Otsuka R. Scr Metall 1976;10:1015.
[32] Asano S, Otsuka R. Scr Metall 1978;12:287.
[33] Abraham DP, Altstetter CJ. Metall Mater Trans A Phys Metall Mater Sci 1995;26:2849.
[34] Borchers C, Michler T, Pundt A. Adv Eng Mater 2008;10:11.
[35] Somerday B, Sofronis P, Jones R. Effects of hydrogen on materials. In: Proc 2008 international hydrogen conference. Materials Park, OH: ASM, International; 2008. p. 779.
[36] Vlasov NM, Zaznoba VA. Phys Solid State+ 1999;41:404.
[37] Chateau JP, Delafosse D, Magnin T. Acta Mater 2002;50:1507.
[38] Chateau JP, Delafosse D, Magnin T. Acta Mater 2002;50:1523.
[39] Yagodzinskyy Y, Hänninen H. Hydrogen–dislocation interactions and their role in help mechanism of hydrogen embrittlement. In: 11th International conference on fracture, Turin; 2005.
[40] Sofronis P, Birnbaum HK. J Mech Phys Solids 1995;43:49.
[41] Sofronis P, Taha A. Environmentally assisted cracking: predictive methods for risk assessment and evaluation of materials. (Eds.), Russell D. Kane Equip Struct 1401, 2000, 70. http://dx.doi.org/10.1520/STP10215S.
[42] Sofronis P, Lufrano J. Mater Sci Eng A Struct Mater Prop Microstruct Process 1999;260:41.
[43] Sofronis P, Liang Y, Aravas N. Eur J Mech A Solids 2001;20:857.
[44] Mao J, McLellan RB. J Phys Chem Solids 2002;63:2029.
[45] Tateyama Y, Ohno T. Phys Rev B 2003;67.
[46] Lu G, Kaxiras E. Phys Rev Lett 2005;94.
[47] Nagumo M. Mater Sci Tech Lond 2004;20:940.
[48] McLellan RB, Xu ZR. Scr Mater 1997;36:1201.
[49] Cuitino AM, Ortiz M. Acta Mater 1996;44:427.
[50] Wen M, Xu XJ, Fukuyama S, Yokogawa K. J Mater Res 2001;16:3496.
[51] Tang YZ, El-Awady JA. Phys Rev B 2012;86.
[52] Matsumoto R, Taketomi S, Matsumoto S, Miyazaki N. Int J Hydrogen Energy 2009;34:9576.
[53] Taketomi S, Matsumoto R, Miyazaki N. J Mater Sci 2008;43:1166.
[54] Schoeck G. Mater Sci Eng A Struct Mater Prop Microstruct Process 2005;400:7.
[55] Hirth JP, Lothe J. Theory of dislocations. New York: Wiley; 1982.
[56] Hull D, Bacon DJ. Introduction to dislocations. 3rd ed. Oxford: Pergamon Press; 1984.
[57] Hestenes MR, Stiefel E. J Res Natl Bureau Standards 1952;49:409.
[58] Hoover WG. Phys Rev A 1985;31:1695.
[59] Nose S. J Chem Phys 1984;81:511.
[60] Swope WC, Andersen HC, Berens PH, Wilson KR. J Chem Phys 1982;76:637.
[61] Finnis MW, Sinclair JE. Philos Mag A Phys Condens Matter Struct Defects Mech Prop 1984;50:45.
[62] Daw MS, Baskes MI. Phys Rev B 1984;29:6443.
[63] Foiles SM, Baskes MI, Daw MS. Phys Rev B 1986;33:7983.
[64] Ramasubramaniam A, Itakura M, Carter EA. Phys Rev B 2009;79.
[65] Voigt W. Lehrbuch der kristallphysik (mit ausschluss der kristalloptik). Leipzig, Berlin: B.G. Teubner; 1910.
[66] Cottrell A. Dislocations and plastic flow in crystals. Oxford: Clarendon Press; 1965.
[67] Cottrell AH, Jaswon MA. Proc R Soc London Ser A Math Phys Sci 1949;199:104.

[68] Zhang F, Curtin WA. Modell Simul Mater Sci Eng 2008;16.
[69] James W, Barnett D. A re-examination of atmospheres and impurity drag on moving dislocations. In: Solute–defect interaction: theory and experiment: proceedings of the international seminar, Kingston, Canada, August 5–9, 1985. Oxford: Pergamon Press; 1986. p. 136.
[70] Haftbaradaran H, Song J, Curtin WA, Gao HJ. J Power Sources 2011;196:361.
[71] Eshelby JD. Proc R Soc London Ser A Math Phys Sci 1957;241:376.
[72] Sofronis P, Birnbaum HK. Fatigue and fracture of aerospace structural materials, vol. 36. American Society of Mechanical Engineers, Aerospace Division; 1993. p. 15.
[73] Dadfarnia M, Sofronis P, Somerday BP, Robertson IM. Int J Mater Res 2008;99:557.
[74] Jagodzinski Y, Hanninen H, Tarasenko O, Smuk S. Scr Mater 2000;43:245.